



# A small change in the surface polarity of cellulose causes a significant improvement in its conversion to glucose and subsequent catalytic oxidation

Magali Hernández <sup>a</sup>, Enrique Lima <sup>a,\*</sup>, Ariel Guzmán <sup>b</sup>, Marco Vera <sup>c</sup>, Omar Novelo <sup>a</sup>, Víctor Lara <sup>c</sup>

<sup>a</sup> Instituto de Investigaciones en Materiales, Universidad Nacional Autónoma de México, Circuito exterior s/n, Cd. Universitaria, Del. Coyoacán, CP 04510 México, D.F., Mexico

<sup>b</sup> ESIQIE-IPN, Departamento de Ingeniería Química – Laboratorio de Investigación en Materiales Porosos, Catálisis Ambiental y Química Fina, UPALM Edif.7 P.B. Zacatenco, México, D.F., 07738, Mexico

<sup>c</sup> Universidad Autónoma Metropolitana, Iztapalapa, Av. San Rafael Atlixco No. 186, Col. Vicentina, CP 09340 México, D.F., Mexico

## ARTICLE INFO

### Article history:

Received 14 February 2013

Received in revised form 27 June 2013

Accepted 26 July 2013

Available online 7 August 2013

### Keywords:

Cellulose

Amino acids

Adsorption

Gold catalysts

Oxidation

## ABSTRACT

Three different amino acids were adsorbed onto the surface of microcrystalline cellulose, which caused changes in the polarity and roughness at the cellulose surface. The adsorptions partially modified the hydrogen bonding network of the cellulose structure, leading to more reactive cellulose residues that were facilely oxidised to gluconic acid by oxygen in the presence of gold zeolite supported catalysts. The conversion of cellulose and the selectivity for gluconic acid was controlled by the identity and amount of amino acid adsorbed onto the cellulose and the extra-framework cation in the zeolite support.

© 2013 Elsevier B.V. All rights reserved.

## 1. Introduction

Cellulose is the largest organic raw material in the world, but many cellulosic products are at present not renewable. Therefore, efforts have been made to convert cellulosic materials into valuable chemicals and renewable fuels [1,2]. The molecular structure of cellulose strongly inhibits its depolymerisation. Cellulose chains are built up from linearly connected anhydroglucopyranose units that are covalently bonded through acetal functions [3,4]. Because of the abundance of hydroxyl groups and oxygen atoms, cellulose is able to form an extensive network of intra- and intermolecular hydrogen bonds, which confers remarkable chemical stability and makes the direct utilisation of cellulose a challenge. One of the promising methods to convert cellulose is heterogeneous catalysis. In this context, acid catalysis has been used to depolymerise cellulose, producing glucose monomers that were converted into bioethanol [5,6] or ethylene glycol [7–9]. Some other efforts for high-temperature pyrolysis or gasification of cellulose to bio-oils

have also been reported [10], but the optimisation of these processes remains incomplete.

The transformation of cellulose under mild conditions into glucose or other molecules that can in turn be converted to chemicals is quite desirable. Therefore, many studies have been focused on the development of an efficient heterogeneous catalyst for the depolymerisation of polysaccharides containing  $\beta$ -1,4-glycosidic linkages [11,12]. Cellobiose, which is a  $\alpha$ -D-glucose dimer connected by a  $\beta$ -1,4-glycosidic bond, has been used as a simple model of cellulose [13]. Of course, there are significant differences between cellobiose and cellulose, but it was assumed that the catalytic conversion of cellobiose may provide helpful insights for the development of efficient routes of cellulose degradation. Thus, some works have reported heterogeneous catalytic conversions of cellobiose by hydrolysis or hydrogenation in an acidic aqueous medium [14,15]. Recently, the oxidative conversion of cellobiose to gluconic acid in the presence of oxygen catalysed by gold nanoparticles loaded on several supports was reported [16,17]. The best results were obtained with a catalyst based on gold nanoparticles in an acidic support. However, the works where cellulose was used instead cellobiose are scarce [18]. This work intends to perturb the hydrogen bonds network of microcrystalline cellulose and then catalytically oxidise the material to gluconic acid in the presence of gold

\* Corresponding author. Tel.: +52 55 5622 4640; fax: +52 55 5616 1371.

E-mail address: [lima@iim.unam.mx](mailto:lima@iim.unam.mx) (E. Lima).

**Table 1**

Elemental analysis of the grafted and ungrafted samples of cellulose.

Code sample	Amount (wt%) of chemical elements			Amount (wt%) of amino acid
	C	O	N	
MC	47.40	52.60	–	–
Ala-MC	47.17	52.32	0.51	3.1
Pro-MC	47.54	52.16	0.30	2.2
PhAla-MC	48.17	51.50	0.33	3.7
Ala-MC-L	47.16	52.57	0.27	1.3
Ala-MC-H	47.79	51.39	0.82	5.0
Ala-MC-VH	47.58	51.17	1.25	7.4
PhAla-MC-L	48.41	51.38	0.21	2.4
PhAla-MC-H	48.48	51.01	0.51	5.6
PhAla-MC-VH	48.56	50.72	0.72	8.2

nanoparticles supported on the acid zeolite HY. It was earlier [19,20] reported that it is possible the substitution of hydroxyl groups in cellulose with small biological molecules, such as amino acids. The grafting of cellulose was accompanied, in general, by the carbamate functionalisation at cellulose surface. To perturb the cellulose surface and pretend to increase its reactivity, in this work amino acids (alanine, proline, and phenyl alanine) were adsorbed onto the cellulose surface, weakening the hydrogen-bond network. The surface polarity of the cellulosic materials was characterised by the adsorption of 3-(4-amino-3-methylphenyl)-7-phenylbenzo-1,2b:4,5b'-difuran-2,6-dione, a solvatochromic molecule [21]. This is a suitable probe because the interaction of the surface environment with a solvatochromic dye is influenced by various interactions, such as acid–base, dipole–dipole and induced dipole–dipole interactions as well as London dispersion forces.

## 2. Experimental procedures

### 2.1. Materials

Proline, phenyl alanine, alanine, microcrystalline cellulose and all solvents were acquired from Sigma–Aldrich (USA).

Microcrystalline cellulose (MC) was hydrothermally treated with an amino acid (alanine, phenyl alanine or proline). Typically, 10 g MC was suspended in 100 mL aqueous solution containing 1 g <sup>13</sup>C-enriched amino acid. The suspension was stirred for 1 h and then refluxed. After 10 min of refluxing, the pH was adjusted to 5 by adding concentrated HCl. Refluxing was continued for 5 h, and the solid was then separated by centrifugation and washed repeatedly until the wash water pH became neutral. The MC functionalised with alanine was named Ala-MC. The samples functionalised with phenyl alanine and proline were labelled PhAla-MC and Pro-MC, respectively, and these compounds were prepared in a similar manner as Ala-MC.

In order to elucidate the effect of the amount of a same amino acid adsorbed on the cellulose surface, two other series of samples were prepared. The first one was prepared in a similar manner as Ala-MC but the amount of alanine was varied, basically a sample with a lower and two with a higher amount of alanine than in Ala-MC were prepared. Sample with the lowest amount of amino acid was named Ala-MC-L and two with higher amount were labelled Ala-MC-H (H for high) and Ala-MC-VH (VH means very high), Table 1. The chemical analysis of the series where the amount of phenyl alanine was varied is also reported in Table 1.

Catalyst Au-HY was prepared from zeolite NH<sub>4</sub>Y (Si/Al ratio of 5.1), which was heated at 400 °C for 6 h to obtain the corresponding protonated HY zeolite. The HY zeolite was suspended in a solution of colloidal Au (5 nm) purchased from Sigma–Aldrich (USA). After 3 h, the solid was separated by centrifugation, repeatedly washed until the wash water was colourless, dried at 50 °C and reduced

at 400 °C under hydrogen flow (10 mL/min) for 4 h. The amount of gold in the catalyst was determined by atomic absorption spectroscopy as 0.8 wt%. This catalyst was named Au-HY. Two other gold-faujasite catalysts were prepared in a similar manner except that the compensating cation was changed using sodium and barium faujasite supports to form Au-NaY and Au-BaY, with a gold loading of 0.93 and 0.97 wt%, respectively.

### 2.2. Characterisation

The cellulose samples were characterised by X-ray photoelectron spectroscopy (XPS), X-ray diffraction (XRD), small angle X-ray scattering (SAXS), and infrared (FTIR) and <sup>13</sup>C nuclear magnetic resonance (MAS NMR) spectroscopy. Changes in polarity at the cellulose surface were characterised by the adsorption of 3-(4-amino-3-methylphenyl)-7-phenylbenzo-1,2b:4,5b'-difuran-2,6-dione dye [22,23] followed by UV–vis spectroscopy.

Catalyst AuY was characterised by XRD, <sup>27</sup>Al and <sup>29</sup>Si MAS NMR and transmission electron microscopy (TEM).

The chemical analysis was obtained using XPS. The analysis was carried out using a VG Microtech ESCA2000 Multilab UHV system, with a Mg K $\alpha$  X-ray source (1253.6 eV) and a CLAM4 MCD analyser. The base pressure during the analysis was  $1.37 \times 10^{-8}$  Pa. The peak positions were referenced to the C 1s hydrocarbon groups in 284.50 eV central peak position. The XPS spectra were fitted with the program SDP v 4.1 [24].

The XRD patterns were acquired using a diffractometer (D8 Advance–Bruker) coupled to a copper anode X-ray tube. K $\alpha$  radiation (40 kV and 30 mA), wavelength of 1.315 Å, was selected with a diffracted beam monochromator. The presence of different crystalline phases was confirmed by fitting the diffraction pattern with the corresponding Joint Committee Powder Diffraction Standards (JCPDS).

A Kratky camera coupled to a copper anode tube was used to measure the SAXS curves. The distance between the sample and the linear proportional counter was 25 cm, and a Ni filter selected for the Cu K $\alpha$  radiation. To perform the measurements, the sample was introduced into a capillary tube. Intensity  $I(h)$  was measured for 9 min to obtain statistical significance. The SAXS data were processed with the ITP program [25–27], where the angular parameter ( $h$ ) is defined as  $h = 4\pi \sin \theta / \lambda$ , where  $\theta$  and  $\lambda$  are the X-ray scattering angle and wavelength, respectively. The obtained data can be described by  $I(q) = \sum_i I_i(0) \exp[-(R_{gi}q)^2/3]$ , where  $I_i(0)$  denotes the scattering intensity at  $q = 0$  of the scattering centre  $i$  with the radius of gyration  $R_{gi}$  [26]. The fractal dimension of the scattering objects was evaluated from the slope of the curve  $\log I(h)$  versus  $\log(h)$  according to the Porod law [28,29].

Mid-infrared (FTIR) spectra were acquired at room temperature using a Perkin Elmer Series spectrophotometer (Model 6X) operated in the ATR-FTIR mode. The spectra were recorded over the 400–4000 cm<sup>-1</sup> spectral window by averaging 32 scans at a maximum resolution of 4 cm<sup>-1</sup>.

<sup>13</sup>C CP MAS NMR spectra were obtained at a frequency of 100.58 MHz using a 4 mm cross-polarisation (CP) MAS probe spinning at a rate of 5 kHz. Typical <sup>13</sup>C CP MAS NMR conditions for <sup>1</sup>H–<sup>13</sup>C polarisation experiment used a  $\pi/2$  pulse of 4  $\mu$ s, contact time of 1 ms and delay time of 5 s. Chemical shifts were referenced to a solid shift at 38.2 ppm relative to TMS.

The morphology of the samples was studied with a SEM Jeol 7600 scanning electron microscope.

The UV–vis absorption maximums of the aminobenzofuran-dione dye adsorbed on the cellulosic materials were recorded in the reflectance mode using a UV–vis spectrometer (Perkin–Elmer Lambda 40). A solution of the solvatochromic probe in 1,2-dichloroethane was added to the cellulose materials. The amount of dye was 0.1 mg per gram of sample.

Low-temperature ( $-130^{\circ}\text{C}$ ) adsorption of CO on reduced Au-Y catalysts was performed. Self-supporting pellets (ca.  $10\text{ mg}/\text{cm}^2$ ) were prepared from the Au-Y samples and treated directly in a specifically designed IR cell connected to a vacuum adsorption apparatus. FTIR spectra were recorded at  $-130^{\circ}\text{C}$  and under outgassing once the samples were warmed to room temperature. Prior to adsorption, the self-supported wafers were outgassed at  $150^{\circ}\text{C}$  for 8 h under vacuum ( $10^{-4}\text{ Torr}$ ).

Gold catalysts were analysed by transmission electron microscopy, in a 120 kV LEO-912AB (ZIES). The TEM images were processed digitally from the negative films by using a film scanner. Size distribution measurements for Au particles were performed on digital images by using the image analysing software Image-Pro.

### 2.3. Catalytic tests

The conversion of cellulose was carried out in a 100 mL Teflon-lined stainless-steel autoclave. Cellulose samples (1 g) and the catalyst (0.05 g) were added into the autoclave pre-charged with  $\text{H}_2\text{O}$  (20 mL). Then, pressurised  $\text{O}_2$  (0.5 MPa) was introduced, and the temperature was increased to  $110^{\circ}\text{C}$  at a rate of  $10^{\circ}\text{C}/\text{min}$  to start the reaction (stirring rate = 400 rpm). After three hours, the liquid products were analysed by HPLC using a Perkin Elmer chromatograph equipped with a refractive index (RI) detector and a Transgenomic™ CARBONSep CHO-620 column.

Mass conversion of cellulose to liquid products was calculated using the following equation:

$$\text{Mass conversion} = 1 - \frac{(\text{Mass of dried solid residue} - \text{Mass of dried catalyst} - \text{Mass of amino acid})}{\text{Initial mass of cellulose}}$$

## 3. Results and discussion

### 3.1. Different amino acids adsorbed on the cellulose surface

Firstly, it has to be mentioned that after the treatment of cellulose with amino acid the wt% of solid material recovered was slightly less than the starting: 99.2% for Ala-MC, 98.9 for PhAla-MC and 97.1 for Pro-MC. This seems contradictory because the cellulose should gain mass due to the adsorption of amino acid. The reaction with amino acids was conducted in HCl at pH 5. Therefore, these aggressive conditions can initiate hydrolysis of cellulose. The following results show that the amino acids were adsorbed at cellulose surface. The amino acid contents of the samples as determined by XPS are reported in Table 1. The amino acid content in the three samples was lower than 5 wt% and the amount did not differ significantly depending of amino acid. Thus, according with other grafting cellulose experiments [30], the percentage of OH groups kinetically available is between 2 and 3%. From Table 1, the amino acid content seems to be random, but is not the case. It is well-known that amino acids are in equilibrium with their zwitterions i.e. their dipolar ions. The isoelectric point is the pH where the concentration of zwitterion is maximal, but of course the pH in general affects the concentration of zwitterion. The isoelectric points for proline, alanine and phenyl alanine are 6.48, 6.01 and 5.48, respectively. Therefore, at the same pH, the ionic species in solution differs for the three amino acids. Thus the interactions ionic–(dipoles)<sub>cellulose</sub> and (dipole)<sub>amino acid</sub>–(dipole)<sub>cellulose</sub> differ and control the amount of amino acid to be adsorbed. The higher the isoelectric point the lower the amount of amino acid adsorbed in cellulose.

The XPS technique was used to evaluate the amino acid content because it is a surface technique and the amino acids were expected to remain adsorbed at cellulose surface. This assumption was confirmed by comparing the surface composition with bulk analysis, where the composition was revealed to be close to that of a glucose carbohydrate with a polymerisation degree of 250. The bulk

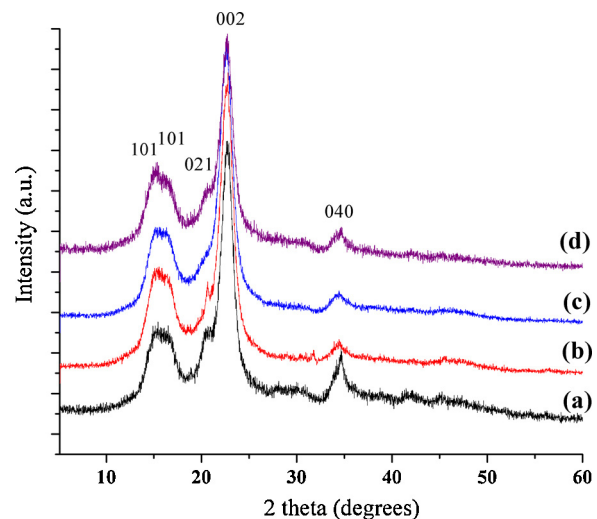


**Fig. 1.** X-ray diffraction patterns of microcrystalline cellulose (a) and microcrystalline cellulose loaded with alanine (b), proline (c) or phenyl alanine (d). Peaks were labelled with the corresponding Miller indexes of crystalline cellulose.

analysis included an assessment of the content of carboxyl groups according to the Tappi standard T 237 om-93 [31]. The content was lower than 0.2 wt%, confirming that the amino acids were mainly adsorbed at the surface.

The XRD patterns of pure cellulose and amino acid–cellulose are displayed in Fig. 1. Amino acid adsorption did not cause the collapse of the crystalline structure of the cellulose. All four XRD patterns presented the typical peaks associated with reported Miller planes for microcrystalline cellulose [32]. However, some minor differences were observed. In samples containing proline and phenyl alanine, the intensity of the (021) plane diminished, suggesting that a preferential orientation in the (002) plane existed. It should be mentioned that XRD is a bulk technique, and no significant differences were expected from the technique in this sample set. A similar result was obtained by FTIR spectroscopy. Fig. 2 shows that no significant differences were observed in the FTIR spectra of pure or amino acid cellulose. The absorption bands attributed to stretching O–H bonds were observed between  $3400$  and  $3200\text{ cm}^{-1}$ . The band close to  $2900\text{ cm}^{-1}$  was caused by stretching C–H bonds. A low intensity band close to  $1600\text{ cm}^{-1}$  was attributed to the  $\delta$  deformation of water molecules. Lastly, the stretching band of C–O bonds was observed at  $1050\text{ cm}^{-1}$ .

The  $^{13}\text{C}$  CP/MAS NMR spectra displayed in Fig. 3 and the peak assignments confirmed the presence of amino acids in the cellulose samples. The peak assignments were made according to the carbon atom numbering on the structures included in Fig. 4. In the MC spectrum (Fig. 3a), all peaks (C1–C6) of the glucose units of cellulose were well resolved. Furthermore, the presence of two broad peaks, marked AC, revealed that a fraction of cellulose was amorphous [33,34].

The Ala-MC spectrum (Fig. 3b) presented peaks at 62, 64, 71, 74, 88 and 104 ppm for cellulose, and peaks for alanine carbons (labelled A-1, A-2 and A-3 according to the structure in Fig. 4) were also observed [35]. The peak for carbon A-3 of pure alanine (spectrum not shown) appeared at 21 ppm, but the peak shifted to 18.7 ppm upon adsorption. Furthermore, the peak for carbon A-3 was more intense than that of carbon A-1, which is the opposite behaviour observed for pure alanine. This result suggests that the relaxation mechanism of the alanine carbons were modified by the interaction between alanine and cellulose, most likely through the

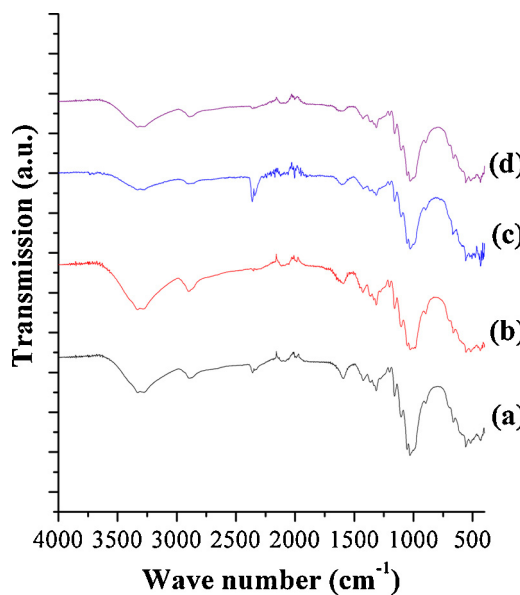


**Fig. 2.** FTIR spectra of microcrystalline cellulose (a) and microcrystalline cellulose loaded with alanine (b), proline (c) or phenyl alanine (d).

hydroxyl groups from cellulose and carbons A-3 and A-1 of alanine. This phenomenon was expected because of the small size of this amino acid.

The peaks of cellulose were well resolved in spectrum for cellulose loaded with proline (Pro-MC, Fig. 3c); however, the proline peaks were not well resolved. They are present in the spectrum (Fig. 3e), but their intensities are very low because this amino acid was not as fully <sup>13</sup>C-enriched. Once again, some peaks presented differences compared to those of the pure amino acid. The chemical shift of carbon P-1 is 173 ppm for pure proline, but the peak shifted downfield to 177 ppm when amino acid was adsorbed to cellulose. A downfield shift was also observed for carbon P-6 to 46 ppm. On the contrary, the NMR peaks of carbons P-3 (24 ppm) and P-4 (29 ppm) were shifted upfield. These observations suggest a noncovalent interaction between proline and cellulose.

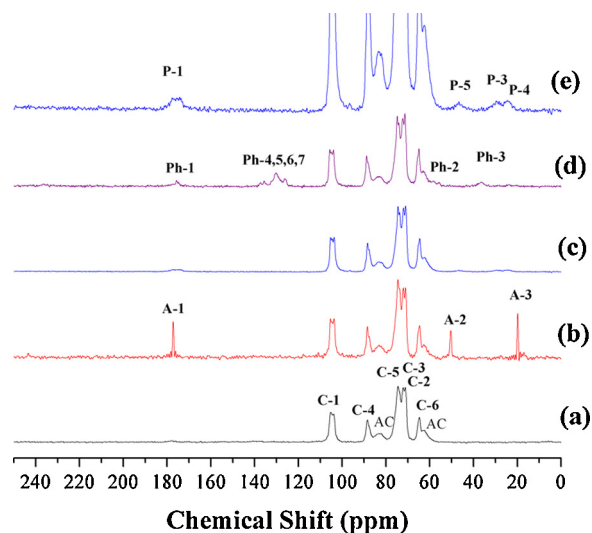


**Fig. 3.** <sup>13</sup>C CP MAS NMR spectra of microcrystalline cellulose (a) and microcrystalline cellulose loaded with alanine (b), proline (c) or phenyl alanine (d). Spectrum (e) is a 6x magnification of spectrum (c). Asterisks indicate spinning side bands (5 kHz).

In the <sup>13</sup>C NMR spectrum of cellulose loaded with phenyl alanine (Fig. 3d), the NMR signals of the amino acid were clearly observed. The chemical shifts of the cellulose carbons C-2 and C-4 (63 and 81 ppm, respectively) were shifted upfield. The NMR peaks corresponding to carbons C-3 and C-5 become broader than the signals observed in pure cellulose. The peaks due to phenyl alanine were well resolved at 35, 56, 125, 129, 131, 136 and 174 ppm. The main difference observed in the peaks of phenyl alanine adsorbed on cellulose and pure phenyl alanine was that the aromatic peaks between 120 and 140 ppm become broader as a consequence of adsorption. Furthermore, a downfield shift was observed for carbons Ph-4, 5, 6 and 7. These observations can be interpreted as the aromatic ring of phenyl alanine interacting with cellulose. The planar structure of the ring could be advantageous for interaction with the cellulose surface. This advantage may be the reason that

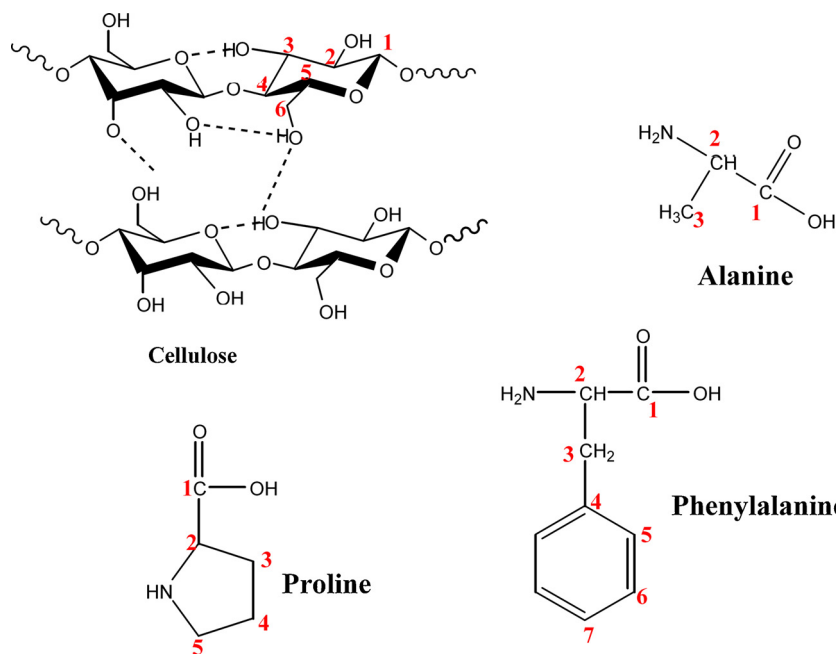


**Fig. 4.** Chemical structure of amino acids and cellulose. Carbon numbering was used for the assignment of NMR signals (spectra in Fig. 3).

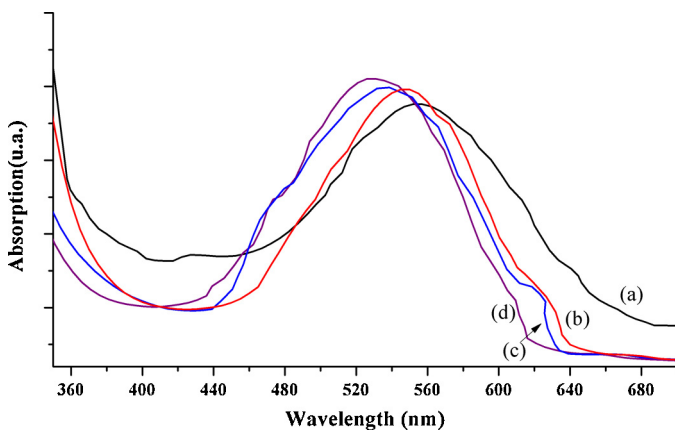


**Fig. 5.** UV/vis absorption spectra of 3-(4-amino-3-methylphenyl)-7-phenylbenzo-1,2b:4,5b'-difuran-2,6-dione adsorbed onto different cellulose samples. (a) MC, (b) Ala-MC, (c) Pro-MC and (d) PhAla-MC.

the amount of phenyl alanine adsorbed onto cellulose was higher than other two amino acids tested.

In summary, structural characterisation showed that alanine, proline, and phenyl alanine could be adsorbed onto a cellulose surface. The amount of amino acid adsorbed onto cellulose was a function of the interactions between the functional groups of amino acids and cellulose. The NMR characterisation qualitatively showed that a perturbation of the cellulose structure occurred when the amino acids were adsorbed.

A relative quantification of the cellulose surface modification was obtained by the adsorption of the polarity indicator [36,37]. Fig. 5 displays the UV-vis reflection spectra of the polarity indicator adsorbed to cellulose samples. The solvatochromic UV-vis absorption band of the dye is due to a  $\pi-\pi^*$  transition [38]. The position of the UV-vis absorption maximum was a function of the chemical composition of the cellulose sample. It is assumed that the adsorbed dye interacts only via the active hydrogen atoms rather than with the lone pair electrons of oxygen atoms at the surface. Thus, the position of the UV-vis absorption maximum observed for the pure cellulose sample can be taken as a reference, and the observed hypsochromic shift in the adsorbed samples (Fig. 5) can be interpreted as a decrease in the hydrogen bond accepting (HBA) capacity of the surface [39,40]. This decrease in HBA capacity depends on the nature of amino acid adsorbed onto cellulose surface. The hypsochromic shift gave the following trend: PheAla-MC > Pro-MC > Ala-MC > MC. This result suggests strong changes in polarity as a consequence of amino acid adsorption. The same trend reflects the degree of modification regarding the polarity of the adsorbed samples, compared to the pure cellulose sample.

The changes in polarity should also cause changes in the textural properties. In this sense, the fractal dimension should be enough to differentiate between the various cellulose samples.

The sample fractal dimension values are reported in Table 2. Lower fractal dimension values correspond to smoother surfaces. MC exhibited the smoothest surface, and, as expected, amino acid adsorption modified the electron density at surface, leading to rougher materials [41,42]. Ala-MC was the least rough of the adsorbed samples. This result agrees with the polarity measurements and can be explained because the interaction of the polar amino acid groups with the surface are not strong enough to significantly perturb the cellulose fibres due to the small size of the amino acid, as suggested by the NMR results. On the contrary, Pro-MC and PhAla-MC had significantly increased roughness measurements compared with MC. In the case of Pro-MC, proline could be interacting with the cellulose surface through its carbonyl group as suggested by the NMR results; therefore, the proline ring or

**Table 2**

Fractal dimension values of cellulose samples as determined by the SAXS data under the Porod law.

Sample	Fractal dimension
MC	2.1
Ala-MC	2.2
Pro-MC	2.4
PhAla-MC	2.7
Ala-MC-L	2.1
Ala-MC-H	2.5
Ala-MC-VH	2.6
PhAla-MC-L	2.5
PhAla-MC-H	2.7
PhAla-MC-VH	2.8

a part of the ring could orient itself perpendicular to the surface, which would significantly increase the roughness of the cellulose. For PhAla-MC, the phenyl alanine could be interacting through the aromatic ring by adsorbing parallel to the (0 0 2) planes of cellulose. These results agree with the XRD results that suggest a preferential (0 0 2) orientation. This orientation would break the hydrogen bonds in the cellulose network, causing a rougher surface. Summarising, SAXS and NMR data show that amino acids adsorb onto the cellulose surface. The level of interaction between amino acid and cellulose, however, is not induced from these analyses. In this context, some SEM images are presented in Fig. 6 where definitely a modification of the surface is shown as a consequence of the adsorption of amino acids. At same scale, the surface of cellulose appears smoother than those containing amino acids. Particularly, with phenyl alanine the surface becomes scaly-like. It should be emphasised that the starting cellulose was microcrystalline and the fibres of the typical cellulose are not well appreciated at this scale.

### 3.2. A same amino acid at different concentration adsorbed on the cellulose surface

The XRD patterns and  $^{13}\text{C}$  CP/MAS NMR spectra of Figs. S1 and S2, respectively (see supplementary material) shows that primary structure of cellulose is not altered as the consequence of the adsorption of low and high amounts of alanine or phenyl alanine. As expected, the XRD pattern of Ala-MC-L is very close to the Ala-MC one. The broad peaks due to cellulose were observed at 15.7°, 22.6° and 34.6°. With an increase of the amount of alanine (samples Ala-MC-H and Ala-MC-VH) some additional narrow XRD peaks were observed at 17°, 28.9°, 30.9° and 34.5°, which should be attributed to the alanine. This behaviour is reproduced for the series of cellulose containing phenyl alanine, with peaks due to this amino acid at 15°, 26.3° and 27.9°. The NMR results agree with those of XRD, the peaks due to cellulose are always observed at 62, 64, 71, 74, 88 and 104 ppm, independently of the amount of amino acid (alanine or phenyl alanine). A high amount of amino acid propitiates that the NMR peaks of alanine or phenyl alanine becomes more intense.

Supplementary data associated with this article can be found, in the online version, at <http://dx.doi.org/10.1016/j.apcatb.2013.07.061>.

The morphological properties are significantly modified by the adsorption at different amount of alanine on the cellulose. The level of modification of surface is a function of the amount of amino acid as shown in SEM images included in Fig. 7. The sample loaded with the lowest amount of alanine (Ala-MC-L) has a relatively smoothed surface. With increase of alanine, the surface exhibits a few amount of crystals well defined, presumably of alanine but the most interesting is that a porous network begins to form and it is well observable for the samples Ala-MC-H and Ala-MC-VH. The size of porous are at nanometric scale but their size is not homogenous and pores ranged between 20 and 100 nm are

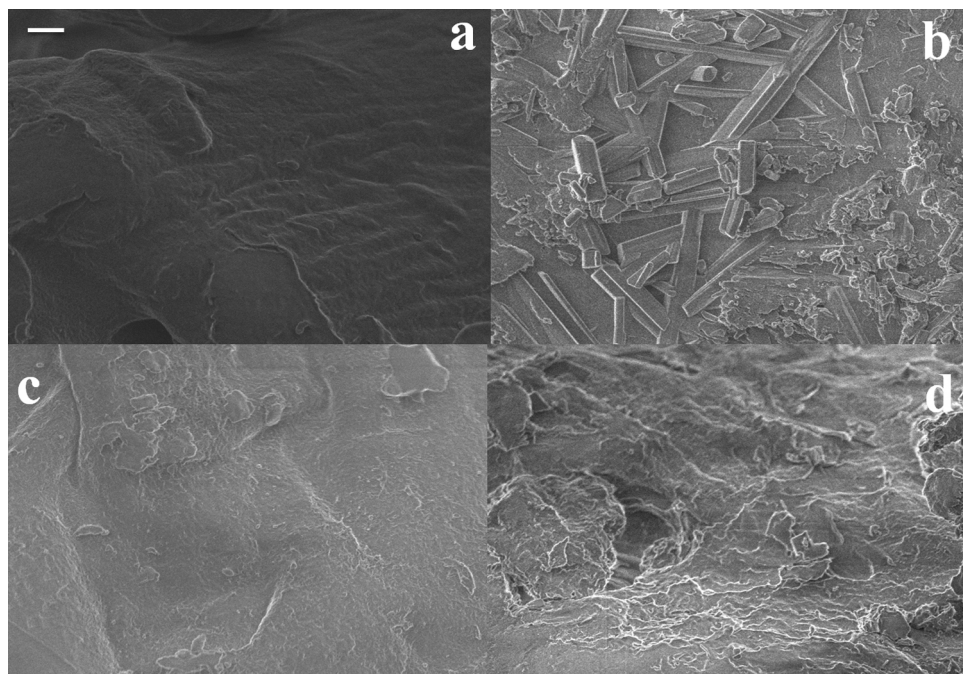


**Fig. 6.** SEM images (10,000×) of microcrystalline cellulose (a) and microcrystalline cellulose loaded with alanine (b), proline (c) or phenyl alanine (d). Bar in the image (a) is equal to 1  $\mu$ m and applicable to four images.

clearly observed. The SEM images for the series where the amount of phenyl alanine was varied follows a similar trend (Fig. S3, supplementary material) as described above for the case of alanine. However, the impact of the phenyl alanine in surface of cellulose is less severe than in the case of alanine.

Supplementary data associated with this article can be found, in the online version, at <http://dx.doi.org/10.1016/j.apcatb.2013.07.061>.

The modifications in the surface revealed by the SEM study are also confirmed by the fractal dimension, Table 2. The higher the amount of amino acid the higher the fractal dimensions. It should be mentioned, however, that the range of the fractal dimension with alanine is wider than those observed in phenyl alanine cellulose samples but the higher values of fractal dimension were reached for the phenyl alanine samples. As above discussed, the fractal dimension should be a parameter measuring the roughness of surface,

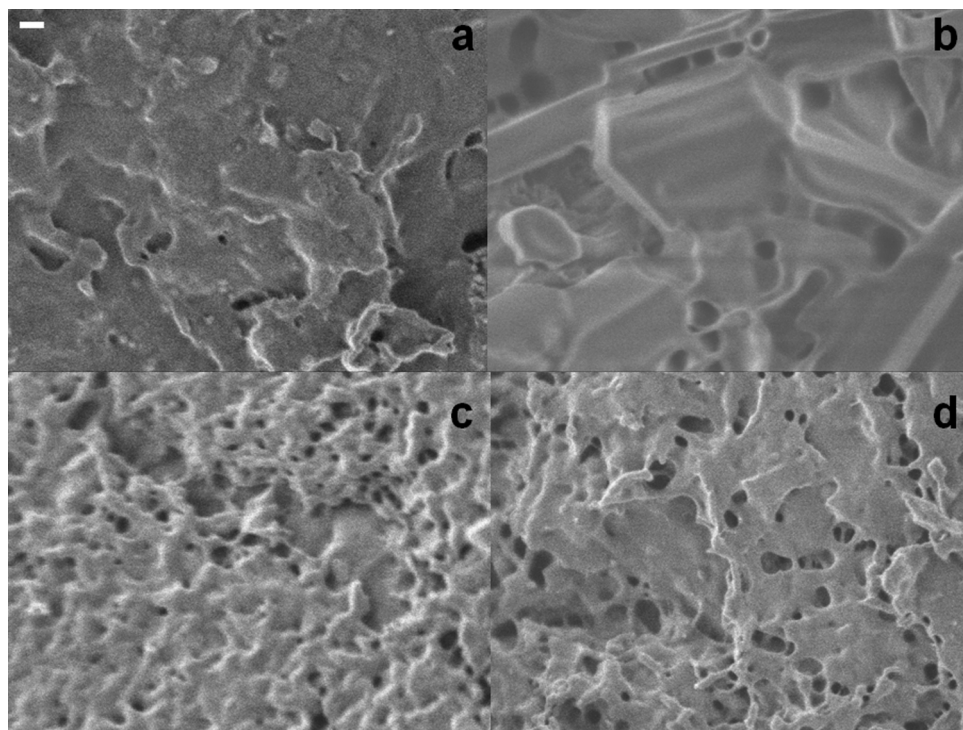


**Fig. 7.** SEM images (50,000×) of cellulose loaded with different amounts of alanine Ala-MC-L (a), Ala-MC (b), Ala-MC-H (c), and Ala-MC-VH (d). Bar in the image (a) is equal to 100 nm and applicable to four images.

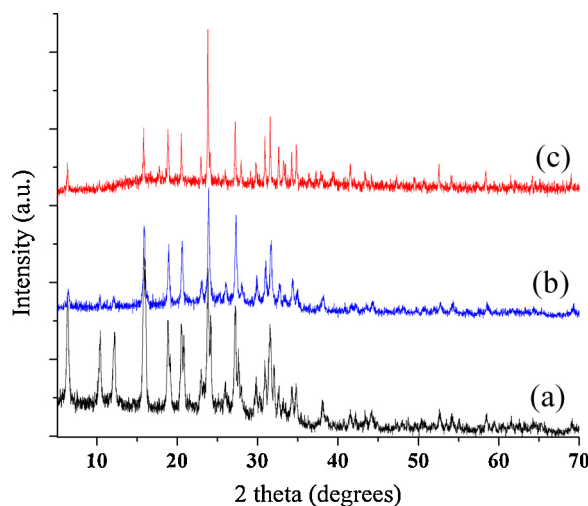


**Fig. 8.** X-ray diffraction pattern of Au-Y catalysts used to oxidise cellulose to gluconic acid. (a) Au-NaY, (b) Au-HY and (c) Au-BaY.

therefore it should be concluded that independently of the amount of amino acid, phenyl alanine is that more harshly modifies the cellulose surface. This same conclusion was reached in Section 3.1 where the nature of amino acid was varied.

### 3.3. Au-Y catalysts

The XRD pattern of the catalysts (Fig. 8) shows that the structure of the faujasite zeolite was maintained after gold loading. The relative intensities of the XRD peaks varied as a function of the compensating cations as the cations occupy the extra-framework positions. This result agrees with the  $^{27}\text{Al}$  and  $^{29}\text{Si}$  MAS NMR spectra (not shown), where no significant differences were observed before and after gold loading. The absence of gold XRD peaks (expected to appear at 37.7, 43.8 and 63.7°) suggests that the gold was well dispersed at the surface of the Au-Y catalysts. TEM showed that the maximal population density of Au particles over the surface was 37 Au particles per  $100\text{ nm} \times 100\text{ nm}$  surface area. The particle size distribution was relatively homogeneous in Au-HY, with a majority of the particles close to 5 nm (Fig. 9). The Au particle size distribution was more heterogeneous on BaY and NaY zeolites, but the average size of the particles was also close to 5 nm.

### 3.4. Catalytic oxidation of amino acid cellulose materials

As stated above, the adsorption of amino acids onto cellulose was conducted under acid conditions, which is indeed a trouble to well understand the catalytic results. Actually, a control experiment was performed where the cellulose without amino acid was treated in HCl and then the corresponding catalytic tests were conducted.

### 3.5. Effect of the nature of amino acid

The oxidation of acid treated cellulose did not occur but, as expected, only a low degree of hydrolysis was observed but the reaction is practically selective only to glucose independently of the catalyst. The absence of oxidation in cellulose can be related to the high crystallinity of this sample if compared to the amino acid–cellulose samples. There is now considerable experimental evidence that the reactivity of cellulose can be increased by partially reducing its crystallinity [5,43]. Therefore, data listed in Table 3 is due purely to cellulose-modified conversion. Some general trends independent of the catalyst were observed. The pure cellulose was practically nonreactive and nonselective. It was demonstrated,

**Table 3**  
Oxidation of cellulose by oxygen in the presence of AuY catalysts.

Catalyst	Code cellulose sample	Cellulose conversion (%)	Selectivity (%)		
			Glucose	Gluconic acid	Other
Au-BaY	MC	2	3	70	27
	MC-acid treated	4	98	1	1
	Ala-MC	22	10	81	9
	Pro-MC	24	5	69	26
	PhAla-MC	33	22	67	11
Au-NaY	MC	2	<1	73	26
	MC-acid treated	5	100	–	–
	Ala-MC	19	11	77	12
	Pro-MC	32	6	50	44
	PhAla-MC	36	49	39	12
Au-HY	MC	3	<1	80	19
	MC-acid treated	6	100	–	–
	Ala-MC	26	13	72	15
	Pro-MC	41	9	57	34
	PhAla-MC	52	58	29	13

however, that amino acid functionalisation of cellulose significantly enhanced its catalytic degradation in the presence of the Au-Y catalysts. Overall, phenyl alanine provided the highest level of cellulose conversion, with Pro-MC exhibiting the second highest and Ala-MC showing the lowest amount of conversion. Conversely, Ala-MC gave the high selectivity for gluconic acid.

The overall catalytic results suggest that the modification of the cellulose surface polarity and roughness significantly altered its reactivity, leading to an increase of the direct catalytic oxidation of cellulose. Nevertheless, the catalyst itself also influenced the selectivity. For instance, PhAla-MC was selectively oxidised to gluconic acid using the Au-BaY catalyst, but this selectivity decreased significantly with Au-NaY and Au-HY, which can be explained by the changes in basicity of the support. In this context, Tan et al. [16] reported yields of 68% of gluconic acid at 81% cellobiose conversion. In fact, it was found that catalysts using basic supports were more selective for gluconic acid than glucose in the oxidation of cellobiose. However, An et al. [18] reported that when oxidative conversion of cellulose into gluconic acid is catalysed by  $\text{Au/Cs}_{3.0-x}\text{PW}_{12}\text{O}_{40}$  similar conversion of cellobiose is reached as reported here with the Au-HY catalyst. However, both catalyst became unstable under hydrothermal conditions. On the one hand, An et al. reported that serious deactivation could be overcome by using  $\text{Au/Cs}_{3.0}\text{PW}_{12}\text{O}_{40}$  in combination with  $\text{H}_3\text{PW}_{12}\text{O}_{40}$ . On the other hand, it is well known that Au-HY under hydrothermal conditions is deactivated because of easy  $\text{H}^+$  leaching. In our case Au-HY became deactivated for the conversion of cellulose during repeated use. Actually in three repeated uses the activity of catalyst decays 50%.

Coming back to data in Table 3, an important observation was that each of the three catalysts was the most selective for gluconic acid using Ala-MC. Furthermore, it should be taken into account that gold particles are most likely stabilised at the external surface of the zeolite because of the particle size, but these surfaces are also influenced by the extra-framework cations. In fact, FTIR spectra of CO adsorbed at a low temperature on Au-HY showed a broad band with a maximum at about  $2142\text{ cm}^{-1}$  and two shoulders at  $2117$  and  $2171\text{ cm}^{-1}$ . These bands have been largely discussed earlier [44–46], and they can be attributed to CO adsorbed linearly on electron deficient Au clusters ( $\text{Au}^{\delta+}$ ), on metallic Au nanoparticles ( $\text{Au}^0$ ) and on surface hydroxyl groups, respectively. The position of the main band correlated with the function of the catalyst, meaning that the electron deficiency depends on the polarisation properties of the compensating cations. Table 4 shows that the position of

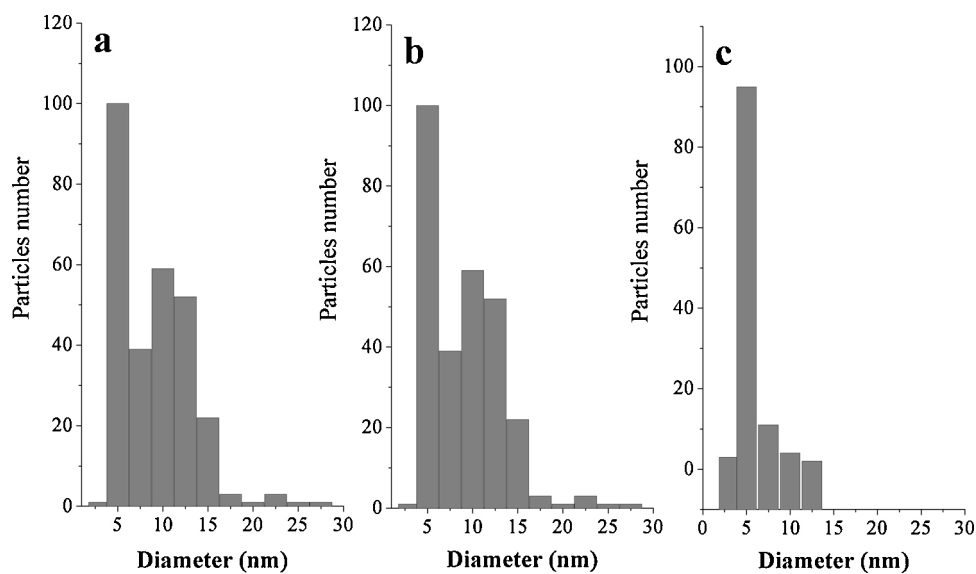


**Fig. 9.** Diameter distribution of Au particles in Au-Y catalysts, as determined by TEM analysis. (a) Au-NaY, (b) Au-BaY and (c) Au-HY.

**Table 4**

Assignment of the FTIR absorption bands of CO adsorbed at  $-130^{\circ}\text{C}$  on Au-Y catalysts.

Code sample	Species/bands ( $\text{cm}^{-1}$ )		
	$\text{CO}\cdots\text{Au}^0$	$\text{CO}\cdots\text{HO}$	$\text{CO}\cdots\text{Au}^{\delta+}$
Au-BaY	2117	2173	2129
Au-NaY	2115	2176	2133
Au-HY	2117	2171	2142

this band is blue shifted in the order  $\text{Ba} < \text{Na} < \text{H}$ , which is the same as the polarising order of these cations. Therefore, the interactions between the polarised surface of cellulose and Au nanoparticles, which are also partially polarised, should be the reason for the selectivity for gluconic acid when the amino acid is small (as in Ala-MC). In this context, the composition of catalyst should be taken into account. Table 5 includes the composition of catalysts-supports and gold content in the catalysts, it is clear that sodium and barium where exchanged in similar percentages in HY parent zeolite. Furthermore, at this level of exchange,  $\text{Ba}^{2+}$  and  $\text{Na}^+$  occur mainly in the large  $\alpha$  cavity. Of course, it should be mentioned that the amount of  $\text{Ba}^{2+}$  and  $\text{Na}^+$  is not enough to saturate the exchange positions in the large cavity [47], in such way that some H remains which provides the acidity to support.

Overall, the best catalyst was Au-HY. Fig. 10 shows that whereas cellulose conversion increases with an increase in both chemical and physical parameters, the glucose selectivity goes in an opposite trend for this catalyst, which confirms that the modifications of the cellulose surface determine the degree of depolymerisation. However, it is unclear that selectivity for gluconic acid was a direct function of the textural parameters. It seems that the amount of amino acid was also a determinant for selectivity. A low selectivity for gluconic acid was obtained for Pro-MC, which was the sample containing the highest amount of amino acid. Thus, the

reactivity depends on the nature and the amount of amino acid at the surface.

After the reaction the amino acid did not remain onto the cellulose residues, as the  $^{13}\text{C}$  CP MAS NMR spectra in Fig. 11 shows. This result suggests that the reaction conditions create the kinetic conditions enough to release amino acid. However, the residues of cellulose could be adsorbed once again in order to be oxidised with the procedure reported in this work.

### 3.6. Effect of the amount of amino acid

As above discussed, the nature of amino acid adsorbed is a variable that changes the reactivity of cellulose. It seems that polarisability and roughness are key parameters that are modified by the amino acid adsorption. Keeping in mind these results, the series of samples where the amount of amino acid was varied were catalytically oxidised by oxygen in the presence of Au-HY catalyst

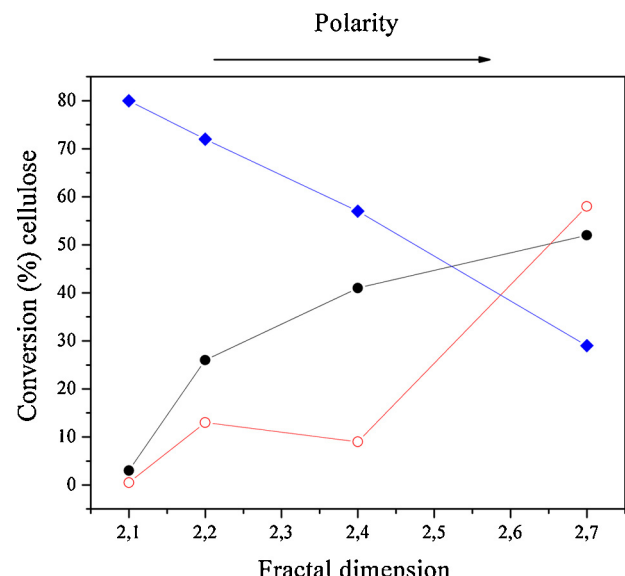


**Fig. 10.** Effect of fractal dimension and polarity on the catalytic performance of Au-HY. Conversion of cellulose (-●-), glucose selectivity (-◆-) and gluconic acid selectivity (-○-).

**Table 5**

Chemical compositions of support-catalysts and content of gold in Au-catalysts.

Code sample	Chemical composition	Au wt% in the Au-Y catalyst
BaY	$\text{Ba}_8\text{H}_{15}(\text{AlO}_2)_{31}(\text{SiO}_2)_{157}\cdot n\text{H}_2\text{O}$	0.97
NaY	$\text{Na}_{22}\text{H}_9(\text{AlO}_2)_{31}(\text{SiO}_2)_{157}\cdot n\text{H}_2\text{O}$	0.93
HY	$\text{H}_{31}(\text{AlO}_2)_{31}(\text{SiO}_2)_{157}\cdot n\text{H}_2\text{O}$	0.80

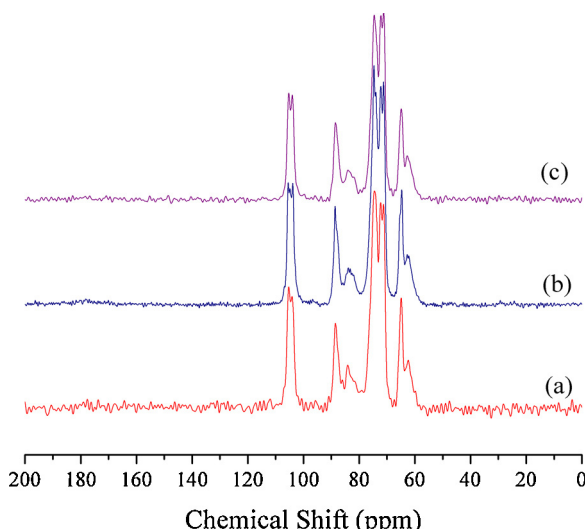


**Fig. 11.**  $^{13}\text{C}$  CP MAS NMR spectra of microcrystalline cellulose loaded with alanine (a), proline (b) or phenyl alanine (c) after the catalytic oxidation tests.

which it was pointed out as the best catalyst in the results described for amino acid–MC series. Table 6 includes the catalytic oxidation results for the complete series of cellulose containing alanine or phenyl alanine. An increase of amino acid, either alanine or phenyl alanine, does not imply necessarily an increase in the catalytic oxidation. The highest activities for these two series of samples were found when amino acid is loaded at moderate concentration (samples Ala-MC, Ala-MC-h, PheAla-MC and PhAla-MC-h). Although the fractal dimension value of the samples increases always with the amount of amino acid, the catalytic activity decays for the highest amount of amino acid which means that cellulose covered by an excess of amino acid cannot be depleted and oxidised. In order to clarify this idea, the cellulose conversion was plotted as a function of the fractal dimension, Fig. 12. Three curves were drawn where one can see that independently of the catalyst used, the cellulose conversion increases monotonically but is not a linear function of the fractal dimension. These three curves correspond to cellulose samples modified with moderate amounts of different amino acids. In contrast, there are two curves where the conversion increases firstly and then decreases. These two curves correspond to cellulose samples loaded with a same amino acid at different concentration. It seems that amino acid amount is determinant to modify the surface but there is an optimal amount of amino acid that assures to reach the most active surface. Amounts as high as 5 and 8 wt% of alanine and phenyl alanine, respectively, on the cellulose surface have a negative effect for degradation of cellulose.

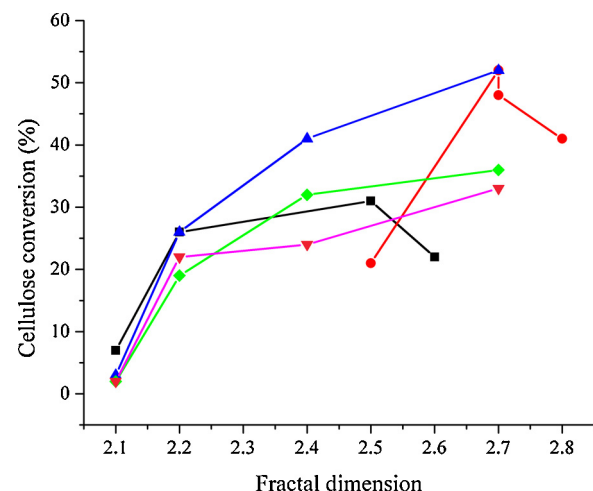


**Fig. 12.** Catalytic activity (cellulose conversion) as a function of the fractal dimension of the cellulose surface. (-▼-) (-◆-) and (-▲-) correspond to cellulose samples with different amino acids catalysed by Au-BaY, Au-NaY and Au-HY, respectively. (-■-) and (-●-) correspond to cellulose samples with different amount of alanine and phenyl alanine, respectively, and catalysed by Au-HY catalyst.

#### 4. Conclusion

The surface of cellulose was modified by the adsorption of alanine, proline and phenyl alanine. Fractal dimension and polarity are parameters that permit the characterisation of the degree of modification induced by amino acid adsorption. Pure and adsorbed cellulose were oxidised by oxygen under mild conditions in the presence of gold-zeolite catalysts. The catalytic activity was determined by both the basicity of catalyst support and the cellulose modification. Adsorbed cellulose was significantly more reactive than pure cellulose. Among the amino acids tested, phenyl alanine gave the most polar, rough and reactive surface. Amount of amino acid is also a key parameter to modify cellulose surface; moderate amounts (3–5 wt%) assures a reactive surface. Au-HY was the most efficient catalyst tested due to electron deficient Au particles.

#### Acknowledgments

The authors would like to acknowledge CONACYT for Grants 128299 and 101319 and PAPIIT-UNAM IN107110. We are also grateful to M. Canseco, G. Cedillo and A. Tejeda for their technical assistance.

#### References

- [1] B. Kamm, *Angewandte Chemie* 119 (2007) 5146–5149.
- [2] L.T. Fan, M. Gharpuray, Y.H. Lee, *Cellulose Hydrolysis*, Springer, Berlin, 1987.
- [3] H.A. Krassig, *Cellulose-structure, Accessibility and Reactivity*, Gordon and Breach Science Publisher, Yverdon, 1993.
- [4] M. Jarvis, *Nature* 426 (2003) 611–612.
- [5] S. Van de Vyver, J. Geboers, P.A. Jacobs, B.F. Sels, *ChemCatChem* 3 (2011) 82–94.
- [6] H. Mehdi, V. Fábos, R. Tuba, A. Bodor, L.T. Mika, I. Horváth, *Topics in Catalysis* 48 (2008) 49–54.
- [7] N. Ji, T. Zhang, M. Zheng, A. Wang, H. Wang, X. Wang, Y. Shu, A.L. Stoltzlemyer, J.G. Chen, *Catalysis Today* 147 (2009) 77–85.
- [8] M.Y. Zheng, A.Q. Wang, N. Ji, J.F. Pang, X.D. Wang, T. Zhang, *ChemSusChem* 3 (2010) 63–66.
- [9] Y. Zhang, A. Wang, T. Zhang, *Chemical Communications* 46 (2010) 862–864.
- [10] J.F. Wishart, *Energy & Environmental Science* 2 (2009) 956–961.
- [11] V. Jollet, F. Chambon, F. Rataboul, A. Cabiac, C. Pinel, E. Guillot, N. Essaïem, *Topics in Catalysis* 53 (2010) 1254–2157.
- [12] C. Luo, S. Wang, H. Liu, *Angewandte Chemie: International Edition* 46 (2007) 7636–7639.
- [13] E.J. Coccino, D.P. Gamblin, B.G. Davis, *Journal of the American Chemical Society* 131 (2009) 11117–11123.
- [14] R. Rinaldi, R. Palkovits, F. Schüth, *Angewandte Chemie* 120 (2008) 8167.
- [15] R. Rinaldi, P. Engel, J. Büchs, A.C. Spiess, F. Schüth, *ChemSusChem* 3 (2010) 1151–1153.

**Table 6**  
Oxidation of grafted cellulose by oxygen in the presence of Au-HY catalyst. Effect of the amount of amino acid.

Code cellulose sample	Cellulose conversion (%)	Selectivity (%)		
		Glucose	Gluconic acid	Other
Ala-MC-L	7	6	65	29
Ala-MC	26	13	72	15
Ala-MC-H	31	11	69	20
Ala-MC-VH	22	17	71	12
PhAla-MC-L	11	42	35	23
PhAla-MC	52	58	29	13
PhAla-MC-H	48	46	30	24
PhAla-MC-VH	39	47	27	26

- [16] X. Tan, W. Deng, M. Liu, Q. Zhang, Y. Wang, *Chemical Communications* 46 (2009) 7179–7181.
- [17] J. Zhang, X. Liu, M.N. Hedhili, Y. Zhu, Y. Han, *ChemCatChem* 3 (2011) 1294–1298.
- [18] D. An, A. Ye, W. Deng, Q. Zhang, Y. Wang, *Chemistry: A European Journal* 18 (2012) 2938–2947.
- [19] D.M. Kalaskar, R.V. Ulijn, J.E. Gough, M.R. Alexander, D.J. Scurr, W.W. Sampson, S.J. Eichhorn, *Cellulose* 17 (2010) 747–756.
- [20] T. Heinze, T. Liebert, *Progress in Polymer Science* 26 (2001) 1689–1762.
- [21] S. Spange, C. Schmidt, H.R. Kricheldorf, *Langmuir* 17 (2001) 856–865.
- [22] I. Devi, P.J. Bhuyan, *Tetrahedron Letters* 46 (2005) 5727–5729.
- [23] S. Spange, R. Sens, Y. Zimmermann, A. Seifert, I. Roth, S. Anders, K. Hofmann, *New Journal of Chemistry* 27 (2003) 520–524.
- [24] SDP v4.1 Copyright® 2004, XPS International, LLC, Compiled 17 January 2004.
- [25] O. Glatter, *Journal of Applied Crystallography* 14 (1981) 101–108.
- [26] O. Glatter, B. Hainish, *Journal of Applied Crystallography* 17 (1984) 435–441.
- [27] O. Glatter, *Progress in Colloid and Polymer Science* 84 (1991) 46–54.
- [28] A. Harrison, *Fractals in Chemistry*, Oxford University Press Inc., New York, 1995.
- [29] I.A. Ibarra, S. Loera, H. Laguna, E. Lima, V. Lara, *Chemistry of Materials* 17 (2005) 5763–5769.
- [30] J.A. Trejo-O'Reilly, J.Y. Cavaille, A. Gandini, *Cellulose* 4 (1997) 305–320.
- [31] TAPPI Standard T 203 om-93, 1993. Alpha-, beta- and gamma-cellulose in pulp and wood. TAPPI Standard T 211 om-93, 1993; Ash in wood, pulp and paper-board: combustion at 525 °C.
- [32] S. Park, J. Baker, M.E. Himmel, P.A. Parilla, D.K. Johnson, *Biotechnology for Biofuels* 3 (2010) 1–10.
- [33] R.H. Newman, *Holzforschung* 58 (2004) 91–96.
- [34] E.L. Hult, T. Liitiä, S.L. Maunu, B. Hortling, T. Iversen, *Carbohydrate Polymers* 49 (2002) 231–234.
- [35] H.O. Kalinowski, S. Berger, S. Braun, *Carbon-13 NMR Spectroscopy*, John Wiley & Sons, New York, 1988.
- [36] S. Spange, A. Reuter, *Langmuir* 15 (1999) 141–150.
- [37] S. Seifert, A. Seifert, G. Brunklaus, K. Hofmann, T. Rüffer, H. Lang, S. Spange, *New Journal of Chemistry* 36 (2012) 674–678.
- [38] C. Laurence, P. Nicolet, M.T. Dalati, J.L.M. Abboud, R.J. Notario, *Physical Chemistry* 98 (1994) 5807–5816.
- [39] K. Fischer, T. Heinze, S. Spange, *Macromolecular Chemistry and Physics* 204 (2003) 1315–1322.
- [40] A.R. Katritzky, D.C. Fara, H. Yang, K. Taemm, T. Tamm, M. Karelson, *ChemInform* 35 (2004) 175–198.
- [41] D. Avnir, D. Farin, P. Pfeifer, *Nature* 308 (1984) 261–263.
- [42] A. Montesinos-Castellanos, E. Lima, J.A. de los Reyes, V. Lara, *Journal of Physical Chemistry C* 111 (2007) 13898–13904.
- [43] J. Geboers, S. Van de Vyver, K. Carpenterier, K. de Blochouse, P. Jacobs, B. Sels, *Chemical Communications* 46 (2010) 3577–3579.
- [44] K. Balakrishnan, A. Sachdev, J. Schwank, *Journal of Catalysis* 121 (1990) 441–455.
- [45] D. Guillemot, V. Yu Borovkov, V.B. Kazansky, M. Polisset-Thfoin, J. Fraissard, *Journal of the Chemical Society, Faraday Transactions* 93 (1997) 3587–3591.
- [46] F. Boucuzzi, A. Chiorino, S. Tsubota, M. Haruta, *Journal of Physics and Chemistry* 100 (1996) 3625–3631.
- [47] W. Breck, *Zeolites Molecular Sieves*, Wiley, New York, 1973.